Video Article

Network Analysis of the Default Mode Network Using Functional Connectivity MRI in Temporal Lobe Epilepsy

Zulfi Haneef[1,2], Agatha Lenartowicz[3], Hsiang J. Yeh[4], Jerome Engel Jr.[4], John M. Stern[4]

[1]Department of Neurology, Baylor College of Medicine

[2]Neurology Care Line, Michael E. DeBakey VA Medical Center

[3]Semel Institute for Neuroscience and Human Behavior, University of California, Los Angeles

[4]Department of Neurology, University of California, Los Angeles

Correspondence to: Zulfi Haneef at Zulfi.Haneef@bcm.edu

URL: https://www.jove.com/video/51442
DOI: doi:10.3791/51442

Keywords: Medicine, Issue 90, Default Mode Network (DMN), Temporal Lobe Epilepsy (TLE), fMRI, MRI, functional connectivity MRI (fcMRI), blood oxygenation level dependent (BOLD)

Date Published: 8/5/2014

Citation: Haneef, Z., Lenartowicz, A., Yeh, H.J., Engel Jr., J., Stern, J.M. Network Analysis of the Default Mode Network Using Functional Connectivity MRI in Temporal Lobe Epilepsy. *J. Vis. Exp.* (90), e51442, doi:10.3791/51442 (2014).

Abstract

Functional connectivity MRI (fcMRI) is an fMRI method that examines the connectivity of different brain areas based on the correlation of BOLD signal fluctuations over time. Temporal Lobe Epilepsy (TLE) is the most common type of adult epilepsy and involves multiple brain networks. The default mode network (DMN) is involved in conscious, resting state cognition and is thought to be affected in TLE where seizures cause impairment of consciousness. The DMN in epilepsy was examined using seed based fcMRI. The anterior and posterior hubs of the DMN were used as seeds in this analysis. The results show a disconnection between the anterior and posterior hubs of the DMN in TLE during the basal state. In addition, increased DMN connectivity to other brain regions in left TLE along with decreased connectivity in right TLE is revealed. The analysis demonstrates how seed-based fcMRI can be used to probe cerebral networks in brain disorders such as TLE.

Video Link

The video component of this article can be found at https://www.jove.com/video/51442/

Introduction

Functional Connectivity MRI (fcMRI) is a relatively recent analytic approach to fMRI data that quantifies the relationship between different brain regions based on the similarity of their blood oxygenation level dependent (BOLD) signal time series – this is called “functional” connectivity, and is distinguishable from anatomical connectivity that describes the existence of physical connections between regions (*e.g.*, white matter fibers). In a special application of this approach, the time series are collected when the participant is not engaged in a task or is in the so-called “resting state”.

Although first described in 1995[1], there has been immense interest in fcMRI resulting in approximately 1,000 publications related to the technique in 2012. fcMRI has intrinsic benefits over task-based fMRI in (1) that there is no specific task to be performed, (2) subject cooperation is not necessary, (3) datasets can be used to query several different networks, (4) better signal to noise ratio is present likely due to differences in cerebral energetics involved, and (5) circumvention of task-related confounds[2]. As a proof of its concept, fcMRI changes have been shown to correspond with changes in EEG[3] and local field potentials[4] in the brain.

Techniques of fcMRI analysis include ROI/ seed-based techniques, independent component analysis (ICA), graph theory analysis, Granger causality analysis, local methods (amplitude of low frequency fluctuations, regional homogeneity analysis), and others[5]. No single technique has yet demonstrated clear superiority over another, although the most popular methods are seed-based and ICA methods[6]. Seed-based fcMRI correlates temporal fluctuations in BOLD signal from a preselected part of the putative network under study termed the “seed” or “region of interest (ROI)” to all other parts of the brain. Areas of the brain showing BOLD signal correlating to the seed area are thought to demarcate parts of the involved network. In contrast, ICA uses a model-free data-driven analysis to extract spatio-temporally correlated brain areas (Independent Components, ICs) by analyzing the hemodynamic signal characteristics of the whole brain[5].

In the current manuscript, a description of methods used in a previously published study of resting state seed-based connectivity analysis of the DMN in TLE is presented[7]. TLE is the most common form of adult epilepsy. In addition to seizures, TLE causes dysfunction of multiple brain networks including memory, behavior, thought, and sensory function[8]. The DMN is constituted by cerebral regions subserving conscious, resting-state cognition. The DMN has been reported to be involved in seizures associated with reduced consciousness[9,10]. Additionally, the hippocampus is the key structure involved in TLE and has been thought to be component of the DMN. However, the connectivity of the PCC to the hippocampal formation is weaker than with other DMN components, such as medial prefrontal and inferior parietal cortices. This suggests that the hippocampus is either a subnetwork of the DMN or an interacting network[11,12]. These commonalities between TLE and DMN raise the possibility that DMN functional connectivity is altered in TLE. This analysis compares the DMN of subjects with TLE to healthy controls to

gain insight into the involvement of DMN in TLE. The connectivity of seeds placed in the chief hubs of the DMN - the anterior and posterior hub regions were analyzed[12]. Seeds were placed in the posterior hub consisting of the retrosplenium/precuneus (Rsp/PCUN) as well as the anterior hub consisting of the ventromedial prefrontal cortex (vmPFC) in patients having TLE and in healthy controls to identify the posterior and anterior subnetworks of the DMN.

Protocol

1. Subjects

1. The study population of 36 subjects includes 3 groups: right TLE (n=11), left TLE (n=12), and healthy controls (n=13). Obtain written informed consent from all subjects. The study follows the guidelines of the University of California, Los Angeles (UCLA) Institutional Review Board.
2. The epilepsy subject groups should be patients who are candidates for anterior temporal lobe resection as determined by video-EEG monitoring, brain MRI, PET imaging, and neuropsychological testing. Patients should continue their usual medications during the fMRI scan and should not be scanned immediately following a seizure. Make sure that all subjects have normal brain MRIs and are free from neurologic illness (other than epilepsy in the patient groups) or are using neurologic medications.

2. Imaging

1. Use a 3 Tesla MRI system for imaging. Obtain axial slices for functional images using an echo planar imaging (EPI) sequence and for anatomic images using a spoiled gradient recalled (SPGR) sequence.
2. Perform functional imaging using the following parameters: TR = 2,000 msec, TE = 30 msec, FOV = 210 mm, matrix = 64 x 64, slice thickness 4 mm, 34 slices. Use the following parameters for high-resolution structural imaging: TR = 20 msec, TE = 3 msec, FOV = 256 mm, matrix = 256 x 256, slice thickness 1 mm, 160 slices.
3. Each imaging session should last 20 min. Ask participants to relax with eyes closed. No special auditory input is required.

3. Preprocessing of BOLD Data

1. Preprocess the fMRI data using FSL (fMRIB Software Library) software version 4.1.6 (Oxford, UK, www.fmrib.ox.ac.uk/fsl)[13,14]. Preprocessing steps should include the following: Use FSL MCFLIRT to remove head movement artifact[15]. Use FSL BET to remove nonbrain tissue[16] with BET option -F for BOLD files. This helps one run further analysis steps on the brain tissue alone.
2. In FEAT, run a minimally processed analysis with registration. Select “First-level analysis” and change “Full analysis” to “Pre-stats” from the top two buttons.
    1. Under Pre-stats tab, uncheck “BET brain extraction” and select “None” for “Motion correction” (as these were already done above). Register the functional (BOLD) images to the anatomical (SPGR) images, and then to a standard (MNI) image. This results in the generation of transformation matrices, which are used later during analysis to warp the seeds selected in standard space into the subject’s brain space.

3. Use the generated transformation matrix (named “standard2example_func.mat”) and transform CSF and white matter ROIs into individual BOLD space.
    1. Extract the time series from the CSF and white matter ROIs using the fslmeants command, using the ROI in individual subject space as a mask. Normalize the extracted time series using the software “R”. These time series are used as regressors in the GLM later to remove the corresponding artifactual signals from the analysis.

4. The next step is removal of subject motion related artifacts. For regression of the motion parameters, set the following within FSL FEAT before running it.
    1. Within the data tab, use motion-corrected and brain-extracted file as inputs, set the TR value to correspond to your dataset. Set high-pass filtering using a 100 sec filter. The high pass filtering will remove signals of no interest, which are of very low frequency. A low pass filter to remove high frequency signals will be applied later in step 4.1.
    2. Within the Pre-stats tab, choose "None" under "Motion correction" as it was already done. Uncheck "BET brain extraction" as it was already done. Perform spatial smoothing using a 5 mm full-width half-maximum (FWHM).
    3. Within the stats tab, regress the 6 motion parameters and their temporal derivatives. Select “None” for convolution and check “Apply temporal filtering.” Use the output of FSL MCFLIRT to get text files of movement parameters, which can be then input into the FEAT analysis model to regress these in a General Linear Model (GLM)
    4. Also add the CSF and white matter signals that were extracted and normalized in previous steps to the GLM. Select “None” for convolution, add temporal derivative, and uncheck “Apply temporal filtering”.

4. Statistical Methods

1. The residuals from preprocessing described above should be used for seed-based correlation. These residuals should be first passed through a low-pass filter of 0.1 Hz, then demeaned by subtracting the mean, dividing by the standard deviation, and then scaled by adding 100. Seeds should be defined with a diameter of 6 mm in the standard MNI space using MRICron software.
2. The posterior and the anterior seeds should correspond to the following coordinates: (1) Rsp/ PCUN region (x=2, y=-60, z=36) and (2) ventromedial prefrontal cortex (vmPFC; x=3, y=60, z=-1). These seed locations have been defined within healthy controls and are transformed to the subject space in the next step[17-19].

1. The seeds should subsequently be transformed to each subject's individual functional brain space from the standard MNI space. For this, use the transformation matrix generated above (named “standard2example_func.mat”) to transform the seed from standard (MNI) space to the individual functional (BOLD) space.
2. Use the fslmeants command to extract the time series from the previously demeaned and scaled residual, using the seed in the individual subject space as a mask. Normalize the extracted time series using the software “R”.

3. Partial correlations between the seed voxels and all other brain voxels should be calculated separately for each subject for each run. For this, within the FSL FEAT GUI, select “First-level analysis”, and then “Stats + Post-stats”. Within the Data tab, the previously demeaned and scaled residual should be used as input into FEAT.
4. Set the High pass filter cutoff to 10,000, as the residual is already high passed at 100 sec. Within the Stats tab, unselect "Use FILM prewhitening", and use the previously extracted and normalized seed time series in the GLM. Within the Post-stats tab, set the desired Z-stat threshold to a value of 2.0.
5. Prior to running group analysis combining runs within subjects, a Fisher's Z transform should be performed on the COPE (Contrast of Parameter Estimates) file generated from the previously run correlation analysis (step 4.3). Copy registration data from the “reg” directory of the FEAT analysis done in step 3.1 into the correlation run of step 4.3.
6. Run a higher-level analysis by combining runs within each subject. For this, within the FSL FEAT GUI, select “Higher-level analysis”, and then “Stats + Post-stats”. Within the “Data” tab, choose "Inputs are lower-level FEAT directories" and enter subject's runs from step 4.4. Within the “Stats” tab, choose “Mixed effects: Simple OLS”. Set up model as mean effect; enter value of 1 for each of the subject's run.
7. To combine data over runs between subjects, an Ordinary Least Squares (OLS) simple mixed effects analysis should be used. For this, within the FSL FEAT GUI, choose”Higher-level analysis”, and “Stats + Post-stats”. Within the Data tab, choose "Inputs are lower-level FEAT directories" and enter subjects' combined runs from step 4.5.
8. Within the Stats tab, choose “Mixed effects: Simple OLS"' Set up a model as 3 groups; enter value of 1 for the group each subject belongs, 0 otherwise. Group analysis should be done on each voxel using a one-way ANOVA with three levels which corresponded to the three groups (right TLE, left TLE, and healthy controls).
9. To threshold the Z statistic images use cluster forming threshold of Z > 2.0 and corrected cluster significant threshold of p=0.05 [20]. To obtain correct z-values on the correlation map, a reverse Fisher's Z transform should be performed on the results.
10. The following specific contrasts should be compared (1) right TLE > controls; (2) left TLE > controls; (3) right TLE > left TLE; (4) left TLE > right TLE; (5) control > right TLE; (6) control > left TLE; (7) TLE (combined right and left) > control; and (7) control > TLE (combined right and left).

Representative Results

Figure 1 shows the DMN revealed with connectivity from a posterior seed (Rsp/ PCUN, red-yellow colors) and an anterior seed (vmPFC, blue-green colors) and compares the networks found in the different subject groups (**Figures 1A-C**) and between each other, namely healthy controls compared to all patients with TLE (**Figures 1D** and **1E**), and then healthy controls compared separately to left TLE (**Figures 1F** and **1G**) and right TLE (**Figures 1H** and **1I**). Direct comparison between left and right TLE is also shown (**Figures 1J** and **1K**).

TLE

TLE includes subjects having either right or left TLE. Compared with controls, this combined group had reduced connectivity from the posterior to the anterior DMN region (**Figure 1D**, red colors) a as well as reduced connectivity from the anterior DMN region to the posterior components (**Figure 1D**, blue colors). Subjects with TLE also showed increased fronto-parietal connectivity with the anterior and posterior DMN (**Figure 1E**, blue/ red colors).

Left TLE

Subjects with left TLE had reduced connectivity of the posterior DMN with the anterior DMN regions and the hippocampus, parahippocampus, brainstem, and medial occipital cortex (**Figure 1F**, red colors). Using an anterior seed, reduced connectivity with posterior components (hippocampus, parahippocampal gyrus, fusiform gyrus, lingual gyrus, cingulate gyrus) was also seen (**Figure 1F**, blue colors). Subjects with left TLE were found to have an expanded peri-opercular network connected to the posterior and anterior seeds (**Figure 1G**, red and blue colors) compared to healthy controls.

Right TLE

As in the case of subjects with left TLE, those with right TLE had reduced connectivity of the posterior DMN seed with the anterior DMN components (**Figure 1H**, red colors). The anterior seed had reduced connectivity to posterior regions (bilateral hippocampus, putamen, caudate) and anterior DMN itself. (**Figure 1H**, blue colors). Areas with increased connectivity of the posterior and anterior seeds in right TLE included left lateral temporal cortex, precuneus, cingulum, and supplementary motor cortex. (**Figure 1I**).

Right vs. Left TLE

Direct comparison of right TLE with left TLE revealed increased connectivity of the posterior DMN seed to the left supramarginal gyrus in left TLE (**Figure 1J**, red colors) as well as the anterior DMN seed to frontal areas (**Figure 1J**, blue colors) compared to right TLE. Areas of increased connectivity of the posterior seed in right TLE included the left hippocampus, fusiform and regions of bilateral thalamus and brainstem. Areas of increased connectivity of the anterior seed in right TLE included precuneus, bilateral thalamic regions, and brainstem regions. (**Figure 1K**).

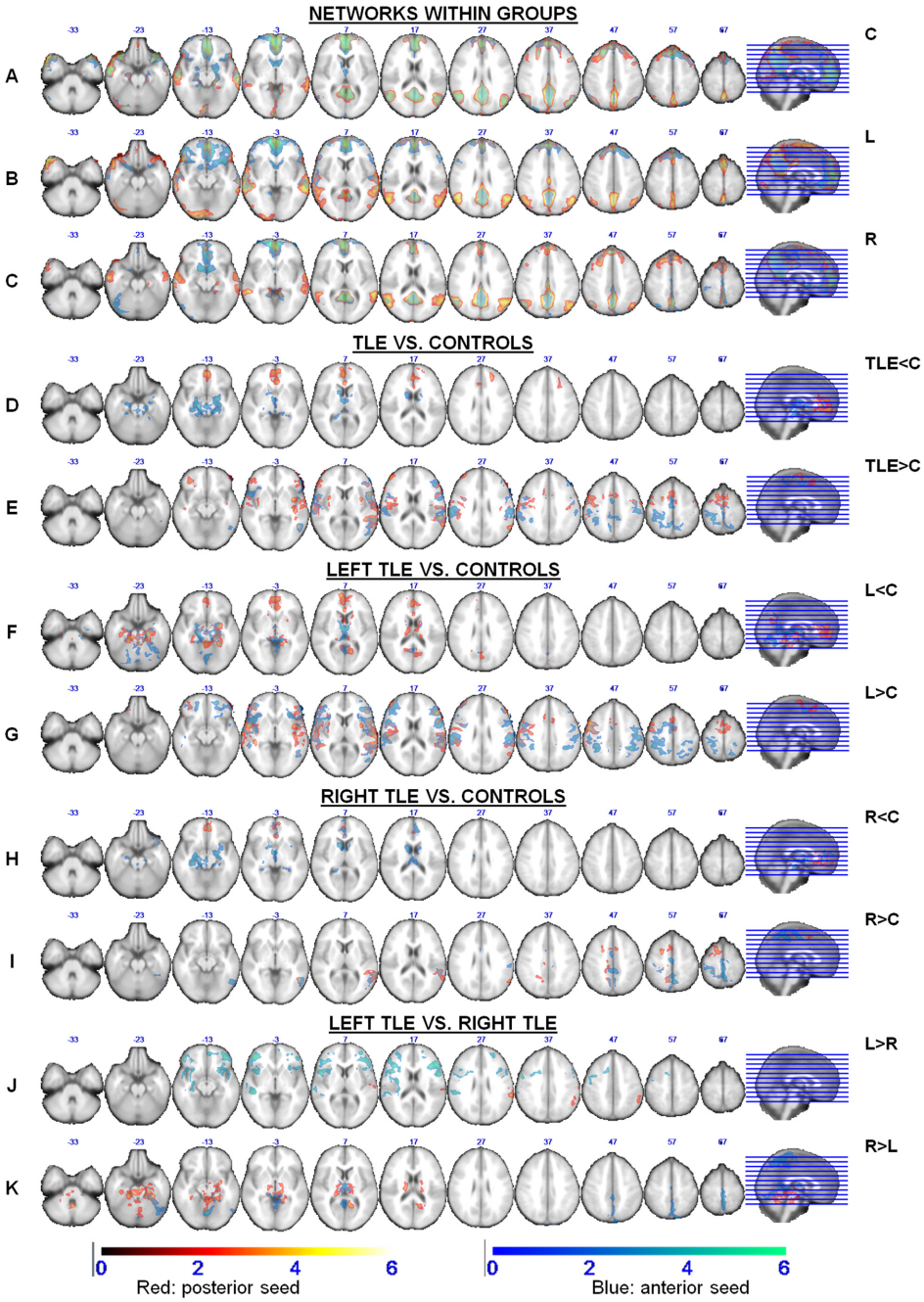

Figure 1. Comparison of DMN in TLE compared to healthy controls. The DMN connectivity using a posterior seed (posterior DMN, Rsp/ PCUN, red-yellow colors) and an anterior seed (vmPFC, blue-green colors) is shown in the different subject groups (**A-C**), TLE compared to healthy controls (**D-E**), left TLE compared to healthy controls (**F-G**), right TLE compared to healthy controls (**H-I**), and right TLE compared to left TLE (**J-K**). C-Control; L-Left TLE; R-Right TLE. Please click here to view a larger version of this figure.

Discussion

Epilepsy is thought to be a network disease, and abnormalities of the involved networks are present during seizures and in the interictal state[21]. Task-based fMRI has been used to analyze abnormalities of the language and memory networks in TLE[8]. FcMRI has inherent advantages in studying the DMN[12] as it is a network mainly active in the resting state. The DMN is a network of brain regions that has been found to be active in awake individuals who are left undisturbed and are engaged in spontaneous thoughts. These regions have been shown to include the vmPFC, Rsp/ PCUN, posterior cingulate cortex, inferior parietal regions, lateral temporal regions, and the hippocampi[12,17]. The DMN is thought to be a substrate for the conscious state. It has been reported to be altered in conditions affecting consciousness, memory, and social cognition such as absence seizures, Alzheimer's disease, and autism/ schizophrenia, respectively[22-26].

The temporal lobe is intricately connected to the DMN. Secondary involvement of the DMN may mediate the effects of TLE on cognition and consciousness[12,27]. Such a secondary involvement of the DMN may also be causative for the clinical effects of other conditions affecting the

temporal lobe/ limbic system such as schizophrenia[25] and Alzheimer's disease[22,26]. Prior studies have shown DMN involvement in TLE and other forms of epilepsy during seizures, during interictal epileptiform discharges, and in the interictal state[9,28-33]. These studies indicate a potentially important role of the DMN in the interictal electrographic and the ictal behavioral characteristics of TLE. In the current experiment, seed-based fcMRI was used to analyze the DMN in TLE in the basal state to evaluate the effect of TLE on the DMN. The hub and spoke model of the DMN posits that its major subsystems are the posterior (Rsp/PCUN) and anterior (vmPFC) components. Here, the connectivity characteristics of these two main regions are individually examined to evaluate how TLE affects their interconnectivity and their associated subnetworks.

The current seed-based analysis reveals a disconnection between the anterior and posterior hubs of the DMN. Such functional connectivity reduction is likely related to a reduction in the anatomical white matter connectivity between the involved structures as has been demonstrated in a study showing simultaneous reduction in functional and white matter connectivity between the posterior DMN and the hippocampus in patients with TLE[34]. Furthermore, it demonstrates generally increased connectivity in left TLE of the anterior and posterior hubs of the DMN to other brain regions and generally decreased connectivity in right TLE. This is consistent with prior studies showing a reduced connectivity in right TLE and compensatory increases of connectivity in left TLE[30,35]. Generally, right TLE tends to involve bilateral structures, whereas left TLE involves redistribution of functional activation[36,37]. This is particularly prominent in the anterior seed where left TLE has a greater connectivity to the peri-opercular areas, compared to right TLE (**Figures 1G, 1I,** and **1J**). This, combined with the lower connectivity of the posterior seed in left TLE compared to controls (**Figures 1F** and **1K**), suggests that the increased anterior connectivity in left TLE could result from a disconnection of the posterior seed or the connections between the posterior and anterior seeds. The hippocampus is connected to the anterior DMN *via* the posterior DMN[34].

The technique used in this study can be modified by changing the seed location and generating brain networks corresponding to other brain areas. Alternative analysis software can be used to do similar analysis (*e.g.*, SPM, AFNI). Seed based correlation analyses are limited in that they require a hypothesis regarding the structure of the putative network under investigation for a prior determination of the seed's location. If the underlying hypothesis is flawed, the results would not be of import.

Resting-state fcMRI[2] can provide a measure of functional connectivity based on spontaneous modulations (*i.e. t*ask unrelated) in BOLD signals. Two commonly used methods for this purpose are seed (region of interest) based correlations and ICA[6]. Seed based correlation analysis requires a hypothesis regarding the structure of the putative network under investigation for a prior determination of the seed's location. After choosing the seed location and extracting the BOLD signal of the voxels constituting the seed, a voxel-by-voxel analysis of the whole brain is performed to identify other brain regions with similar BOLD signal patterns, and this elucidates a correlated network. Another method of seed analysis is by correlating the signal between two, or multiple, regions of interest. Using such a method, the connectivity was found to be reduced between the lesional hippocampus and the posterior DMN in TLE[38]. On the other hand, ICA is data driven without a pre-existing hypothesis and delineates spatio-temporally distinct networks within the resting state brain. A study of DMN in TLE has also been performed using ICA and determined reduced connectivity of the anterior DMN in patients with right and left TLE compared to controls. However, our ROI (seed)-based analysis showed the presence of an anterior DMN network in TLE, which was actually more extensive in left TLE compared to control subjects. This discrepancy could be related to the proposed disconnection of the anterior from posterior DMN, where a separated anterior network is less visible when evaluating a network identified primarily by the posterior DMN connections. In agreement with a prior study, we could replicate the mesial temporal involvement in TLE[39].

The current analysis shows how seed-based fcMRI can be used to probe cerebral networks in brain disorders such as TLE. Identification of such group differences helps understand the functional abnormalities in disease states opening the possibility of future applications that implement analyses that can be interpreted at the single subject level[2].

One limitation of this analysis is the inability to determine the awake/asleep state of the subject. Sleep has been associated with reduced DMN connectivity of the frontal cortex with deep sleep[40] or with general anesthesia[41]. Further investigation is warranted to explore whether these findings can be reproduced by controlling for sleep state.

Critical steps within the protocol described here include the following: a) preprocessing steps; b) identification of seed location; c) extracting time-course of the specified seed(s); d) correlating the above time-course to the remaining brain voxels; e) generating maps of correlated brain areas to visualize the brain network corresponding to the specified seed; and f) comparison of brain network maps thus generated to look for group differences in the seed networks.

Disclosures

Dr. Engel is funded by NIH Grants P01 NS02808, R01 NS33310, and U01 NS42372, has patents WO 2009/123734A1, and WO 2009/123735A1, receives royalties from MedLink, Wolters Kluwer, Blackwell, and Elsevier, and has received honoraria from Medtronics, Wolters Kluwer, and Best Doctors. Dr. Stern has served as a paid consultant for UCB and Lundbeck. Dr. Stern is an editor of MedLink Neurology, and has received royalties from Wolters Kluwer and from McGraw-Hill. The remaining authors have no disclosures or conflicts of interest to declare.

Acknowledgements

Funding for this research was provided by The Epilepsy Foundation of America, Baylor College of Medicine Computational and Integrative Biomedical Research Center (CIBR) Seed Grant Awards (ZH); NIH-NINDS K23 Grant NS044936 (JMS); and The Leff Family Foundation (JMS). Data acquisition was assisted by: Elizabeth Pierce (UCLA).

References

1. Biswal, B. B., Yetkin, F. Z., Haughton, V. M., & Hyde, J. S. Functional connectivity in the motor cortex of resting human brain using echo-planar MRI. *Magn. Reson. Med.* **34**, 537-541 (1995).

2. Fox, M. D., & Greicius, M. Clinical applications of resting state functional connectivity. *Front. Syst. Neurosci.* **4**, 1-13 (2010).
3. Laufs, H. *et al.* Electroencephalographic signatures of attentional and cognitive default modes in spontaneous brain activity fluctuations at rest. *Proc. Natl. Acad. Sci. U.S.A.* **100**, 11053-11058, doi:10.1073/pnas.1831638100 (2003).
4. Shmuel, A., & Leopold, D. A. Neuronal correlates of spontaneous fluctuations in fMRI signals in monkey visual cortex: Implications for functional connectivity at rest. *Hum. Brain Mapp.* **29**, 751-761, doi:10.1002/hbm.20580 (2008).
5. Margulies, D. S. *et al.* Resting developments: a review of fMRI post-processing methodologies for spontaneous brain activity. *Magn. Res. Mater. Phys. Biol. Med.* **23**, 289-307 (2010).
6. Biswal, B. B. *et al.* Toward discovery science of human brain function. *Proc. Natl. Acad. Sci. U.S.A.* **107**, 4734-4739, doi:10.1073/pnas.0911855107 (2010).
7. Haneef, Z., Lenartowicz, A., Yeh, H. J., Engel, J., Jr., & Stern, J. M. Effect of lateralized temporal lobe epilepsy on the default mode network. *Epilepsy Behav.* **25**, 350-357, doi:10.1016/j.yebeh.2012.07.019 (2012).
8. Pillai, J. J., Williams, H. T., & Faro, S. Functional imaging in temporal lobe epilepsy. *Semin. Ultrasound. CT MR.* **28**, 437-450 (2007).
9. Blumenfeld, H. *et al.* Positive and negative network correlations in temporal lobe epilepsy. *Cereb. Cortex.* **14**, 892-902, doi:10.1093/cercor/bhh048 (2004).
10. Dupont, P. *et al.* Dynamic perfusion patterns in temporal lobe epilepsy. *Eur. J. Nucl. Med. Mol. Imaging.* **36**, 823-830, doi:10.1007/s00259-008-1040-6 (2009).
11. Fransson, P., & Marrelec, G. The precuneus/posterior cingulate cortex plays a pivotal role in the default mode network: Evidence from a partial correlation network analysis. *Neuroimage.* **42**, 1178-1184, doi:10.1016/j.neuroimage.2008.05.059 (2008).
12. Buckner, R. L., Andrews-Hanna, J. R., & Schacter, D. L. The brain's default network. *Ann. N. Y. Acad. Sci.* **1124**, 1-38 (2008).
13. Woolrich, M. W., Ripley, B. D., Brady, M., & Smith, S. M. Temporal autocorrelation in univariate linear modeling of FMRI data. *Neuroimage.* **14**, 1370-1386, doi:10.1006/nimg.2001.0931 (2001).
14. Forman, S. D. *et al.* Improved assessment of significant activation in functional magnetic resonance imaging (fMRI): use of a cluster size threshold. *Magn. Reson. Med.* **33**, 636-647 (1995).
15. Jenkinson, M., Bannister, P., Brady, M., & Smith, S. Improved optimization for the robust and accurate linear registration and motion correction of brain images. *Neuroimage.* **17**, 825-841 (2002).
16. Smith, S. M. Fast robust automated brain extraction. *Hum. Brain Mapp.* **17**, 143-155, doi:10.1002/hbm.10062 (2002).
17. Raichle, M. E. *et al.* A default mode of brain function. *Proc. Natl. Acad. Sci. U.S.A.* **98**, 676-682 (2001).
18. Uddin, L. Q., Kelly, A. M., Biswal, B. B., Castellanos, F. X., & Milham, M. P. Functional connectivity of default mode network components: correlation, anticorrelation, and causality. *Hum. Brain Mapp.* **30**, 625-637, doi:10.1002/hbm.20531 (2009).
19. Singh, K. D., & Fawcett, I. P. Transient and linearly graded deactivation of the human default-mode network by a visual detection task. *Neuroimage.* **41**, 100-112, doi:10.1016/j.neuroimage.2008.01.051 (2008).
20. Worsley, K. J., Evans, A., Marrett, S., & Neelin, P. A three-dimensional statistical analysis for CBF activation studies in human brain. *J. Cereb. Blood Flow Metab.* **12**, 900-918 (1992).
21. Spencer, S. S. Neural networks in human epilepsy: evidence of and implications for treatment. *Epilepsia.* **43**, 219-227 (2002).
22. Greicius, M. D., Srivastava, G., Reiss, A. L., & Menon, V. Default-mode network activity distinguishes Alzheimer's disease from healthy aging: evidence from functional MRI. *Proc. Natl. Acad. Sci. U.S.A.* **101**, 4637-4642, doi:10.1073/pnas.0308627101 (2004).
23. Kennedy, D. P., Redcay, E., & Courchesne, E. Failing to deactivate: resting functional abnormalities in autism. *Proc. Natl. Acad. Sci. U.S.A.* **103**, 8275-8280 (2006).
24. Garrity, A. G. *et al.* Aberrant "default mode" functional connectivity in schizophrenia. *Am. J. Psychiatry.* **164**, 450-457, doi:10.1176/appi.ajp.164.3.450 (2007).
25. Mannell, M. V. *et al.* Resting state and task-induced deactivation: A methodological comparison in patients with schizophrenia and healthy controls. *Hum. Brain Mapp.* **31**, 424-437, doi:10.1002/hbm.20876 (2010).
26. Jones, D. *et al.* Age-related changes in the default mode network are more advanced in Alzheimer disease. *Neurology.* **77**, 1524-1531 (2011).
27. Kobayashi, Y., & Amaral, D. G. Macaque monkey retrosplenial cortex: II. Cortical afferents. *J. Comp. Neurol.* **466**, 48-79 (2003).
28. Dupont, P. *et al.* Dynamic perfusion patterns in temporal lobe epilepsy. *Eur. J. Nuclear Med. Mol. Imaging.* **36**, 823-830 (2009).
29. Laufs, H. *et al.* Temporal lobe interictal epileptic discharges affect cerebral activity in “default mode” brain regions. *Hum. Brain Mapp.* **28**, 1023-1032 (2007).
30. Morgan, V. L., Gore, J. C., & Abou-Khalil, B. Functional epileptic network in left mesial temporal lobe epilepsy detected using resting fMRI. *Epilepsy Res.* **88**, 168-178 (2010).
31. Gotman, J. *et al.* Generalized epileptic discharges show thalamocortical activation and suspension of the default state of the brain. *Proc. Natl. Acad. Sci. U.S.A.* **102**, 15236-15240, doi:10.1073/pnas.0504935102 (2005).
32. Hamandi, K. *et al.* EEG-fMRI of idiopathic and secondarily generalized epilepsies. *Neuroimage.* **31**, 1700-1710 (2006).
33. Pittau, F., Grova, C., Moeller, F., Dubeau, F., & Gotman, J. Patterns of altered functional connectivity in mesial temporal lobe epilepsy. *Epilepsia.* **53**, 1013-1023, doi:10.1111/j.1528-1167.2012.03464.x (2012).
34. Liao, W. *et al.* Default mode network abnormalities in mesial temporal lobe epilepsy: a study combining fMRI and DTI. *Hum. Brain Mapp.* **32**, 883-895, doi:10.1002/hbm.21076 (2011).
35. Pereira, F. R. *et al.* Asymmetrical hippocampal connectivity in mesial temporal lobe epilepsy: evidence from resting state fMRI. *BMC Neurosci.* **11**, 1-13, doi:10.1186/1471-2202-11-66 (2010).
36. Dupont, S. *et al.* Bilateral hemispheric alteration of memory processes in right medial temporal lobe epilepsy. *J. Neurol. Neurosurg. Psychiatr.* **73**, 478-485 (2002).
37. Vlooswijk, M. C. *et al.* Functional MRI in chronic epilepsy: associations with cognitive impairment. *Lancet Neurol.* **9**, 1018-1027, doi:10.1016/S1474-4422(10)70180-0 (2010).
38. McCormick, C., Quraan, M., Cohn, M., Valiante, T. A., & McAndrews, M. P. Default mode network connectivity indicates episodic memory capacity in mesial temporal lobe epilepsy. *Epilepsia.* **54**, doi:10.1111/epi.12098 (2013).
39. Zhang, Z. *et al.* Altered spontaneous neuronal activity of the default-mode network in mesial temporal lobe epilepsy. *Brain Res.* **1323**, 152-160, doi:10.1016/j.brainres.2010.01.042 (2010).
40. Horovitz, S. G. *et al.* Decoupling of the brain's default mode network during deep sleep. *Proc. Natl. Acad. Sci. U.S.A.* **106**, 11376-11381, doi:10.1073/pnas.0901435106 (2009).

41. Deshpande, G., Kerssens, C., Sebel, P. S., & Hu, X. Altered local coherence in the default mode network due to sevoflurane anesthesia. *Brain Res.* **1318**, 110-121, doi:10.1016/j.brainres.2009.12.075 (2010).

